Clay mineral expansion of black cotton soil based on interlayer cation hydration

Cheng Yongzhen[1, 2]   Huang Xiaoming[1]

(¹ School of Transportation, Southeast University, Nanjing 210096, China)
(² Faculty of Architecture and Civil Engineering, Huaiyin Institute of Technology, Huai'an 223001, China)

Abstract: To analyze the water swelling characteristics of black cotton soil (BCS), X-ray fluorescence and X-ray diffraction characterizations were performed to investigate the chemical compositions and types of clay minerals in BCS. A montmorillonite crystal lattice was established to simulate the hydration of interlayer cations by applying the SPC/E potential energy model, universal force field, algorithm of charge balance, and periodic boundary. Results indicated that the main clay mineral found in the BCS was montmorillonite (32. 6%) with small amounts of interstratified illite-montmorillonite (10. 9%), illite (2. 3%), and kaolinite (1.5%). The high expansive potential of BCS comes from the strong adsorption property of montmorillonite with a high content of magnesium and sodium ions to water molecules. The exchangeable cations of Na^+ in BCS were only 3. 73% , but they enhanced the adsorption capacity of clay to water molecules and accelerated the hydration of Mg^{2+} (47. 1%) and Ca^{2+} (4. 78%). The free swell index can be used as a classification index of the swelling potential of BCS.
Key words: black cotton soil; swelling characteristics; clay minerals; molecular simulation; interlayer cation hydration
DOI: 10. 3969/j. issn. 1003 − 7985. 2021. 03. 010

B lack cotton soil (BCS) has been found in abundance in Eastern Africa, and similar clays also abound in other places such as South Asia, Australia, and China[1]. Nairobi, the capital of Kenya, is located in the Robe Valley in Central Africa, where about 60% of the surface is covered by BCS. The soils are highly expansive when exposed to water during the rainy season[2–3]. However, the expansion seems to vanish during the following dry season[4–5]. The swelling pressure of BCS in Nairobi was reported to be 8-10 kg/cm², and the volume change is as large as 120% -300% . These properties bring about serious problems in light construction on BCS. Iterative

swelling-shrinkage and low bearing capacity always cause soil weakness and result in damage to highways such as slope failure, subgrade settlement, and pavement cracking. To find a strategy to overcome these problems for highway construction, the clay minerals in Nairobi BCS and their water swelling properties must be investigated.

Scientific mineral identification techniques have been developed in the last decade. Methods such as chemical analysis, X-ray diffraction (XRD) characterizations, differential thermal analysis, thermogravimetric analysis, infrared spectral absorption, and polarized light microscope plus microscopic analysis are commonly used[6]. Extensive research has been conducted on mineralogical identification of clay minerals by explaining diffraction data[7]. However, few reports on Nairobi BCS have been found in the field of mineralogical quantification for unknown reasons. The types of clay minerals in soils can be determined by comparing the XRD pattern with standard minerals. The potential for using XRD-based techniques for the quantification of clay minerals on the basis of identified phases has been investigated[8–9].

The swelling properties of clay minerals have been researched using experimentation and molecular simulation to investigate hydration, interlayer structure, and dynamics of interlayer positive ions in the clay[10–11]. The experimental techniques present a few limitations in exploring the microstructure. Molecular simulation has been regarded as a valuable tool for addressing unsolved issues related to clay swelling as a complement to experimental techniques. Molecular simulation directly employs structural information to investigate structure-function relationships. Nonequilibrium states related to expansive hysteresis may be studied systematically by using computational methods. Molecular simulation allows for research on sophisticated clay systems by using simplified conditions, e. g., the behavioral information of the individual interlayers can be acquired without complexities from the mixing layer hydrate formation or disturbance from outside surface effects.

In this research, experimental investigation and molecular simulation were revisited and used to identify the types of the clay minerals and explain the hydration of the interlayer irons to reveal the swelling properties of Nairobi BCS. The chemical constituent and XRD patterns were

used to determine the types of the clay minerals and predict the percentages of various clay minerals. The adsorption of water molecules was simulated to analyze the combinative capabilities of the interlayer Na^+, Ca^{2+}, or Mg^{2+} ions with water. The hydration of the interlayer irons was also investigated to explain the strong expansion characteristics of Nairobi BCS. To confirm the classification standard of the expansive potential of BCS by using free swell index (FSI) as an indicator, the FSI test was performed and the correlation of FSI with the montmorillonite content and cation exchange capacity (CEC) of Nairobi BCS was investigated.

1　Materials and Experimental Methods

1.1　BCS sampling sites and pretreatments

BCS was sampled from a roadbed site in Nairobi, Kenya ($36°31'$E, $1°35'$S), where a beltway called the Southern Bypass was being built by China Road and Bridge Co. The natural BCS is characterized by darkness and cracking, as shown in Fig.1. The samples were first cut into slices and air-dried for several days and then ground in a mortar until all soil particles passed through a 2.0 mm sieve. The soil particles with different sizes, such as clay (< 2 μm), silt (2-75 μm), and sand (75 μm-2.0 mm), were obtained in accordance with the standard method[12]. BCS consisted of 52% clay and 48% silt. The free swell ratio (FSR) of BCS was 165%, and the liquid limit and plasticity index were 57% and 26%, respectively, which indicates that BCS belongs to clay with high plasticity and expansive potential on the basis of JTG E40—2007[12].

Fig. 1　Typical morphological characteristics of black cotton soil

1.2　Mineral phase analysis

The mineral phases were determined by XRD performed on BCS in accordance with the Chinese standard[13]. The BCS was first oven-dried until a constant weight was achieved at 60 ℃ and was ground in a mortar to make all soil particles less than 40 μm. The specimens were made by pouring the powders into a sample frame and pressing them in a vertical direction. The diffracto-

grams were obtained by fixing the specimens on the holder of the XRD diffractometer (Ultima Ⅳ, CuKα radiation). Data were then recorded at a speed of 2(°)/min per step. X-ray fluorescence (XRF) was performed on a Thermo ADVANT'XP instrument to inspect the chemical composition of BCS.

1.3　FSI test

The FSI of BCS was determined in accordance with JTG E40—2007. The air-dried BCS was ground in a mortar until all soil particles passed through a 0.5 mm sieve opening. The soil samples were oven-dried at 105 ℃ until a constant weight was achieved then cooled down to room temperature in a dryer. Then, 10 g of soil was weighed and poured into a 50 mL measuring cylinder with 30 mL of distilled water. The mixture in the cylinder was stirred ten times from the liquid surface to the bottom of the cylinder by using a stirring rod. Then, the soil particles on the stirring rod and the inner surface of the cylinder were washed into the measuring cylinder until the liquid surface reached 50 mL. After standing for 24 h, the equilibrium sediment volume was noted. Distilled water was replaced with kerosene, and the same operational approaches were performed to obtain the equilibrium sediment volume of 10 g oven-dried soil passing a 0.5 mm sieve in kerosene. The FSR and the FSI can be calculated as

$$\delta_{FSR} = \frac{V_d - V_0}{V_0} \times 100\% \qquad (1)$$

$$\delta_{FSI} = \frac{V_d - V_k}{V_k} \times 100\% \qquad (2)$$

where δ_{FSR} is the free swell ratio of BCS; δ_{FSI} is the free swell index of BCS; V_0 is the volume of the 10 g oven-dried soil; V_d is the equilibrium sediment volume of 10 g oven-dried soil passing a 0.5 mm sieve in distilled water; and V_k is the equilibrium sediment volume of 10 g oven-dried soil passing a 0.5 mm sieve in kerosene.

2　Molecular Mechanics Simulation

2.1　Potential energy model

The potential energy reflects the interatomic potentials between atoms or ions and can be simulated by the SPC/E model, which provides a good description of the balance, structure, and kinetic behavior of water. This model supposes every water molecule has three interactional potentials at the location of an atomic nucleus, the bond length of O-H is 0.1 nm, and the bond angle of H-O-H is 109.47°. Van der Waals force is described by the potential energy of Lennard-Jones (LJ) as follows:

$$V(r_{ij}) = 4\varepsilon_{ij}\left[\left(\frac{\sigma_{ij}}{r_{ij}}\right)^{12} - \left(\frac{\sigma_{ij}}{r_{ij}}\right)^{6}\right] + \frac{q_i q_j}{4\pi\varepsilon_0 r_{ij}} \qquad (3)$$

where q_i and q_j are the charges on the atoms i and j, respectively; r_{ij} is the distance between atoms i and j; and ε_o is the dielectric constant. The LJ cross-interaction terms, ε_{ij} and σ_{ij}, are generated from the standard combining relationships,

$$\sigma_{ij} = \frac{\sigma_i + \sigma_j}{2} \tag{4}$$

$$\varepsilon_{ij} = \sqrt{\varepsilon_i \varepsilon_j} \tag{5}$$

2.2 Model construction

The model parameters come from Wyoming montmorillonite. The crystal texture of the montmorillonite is a clinorhombic system, and the space groups are C2/m. The octahedral coordination cations are located on the two sides of the symmetry plane. The cell parameters are as follows: $a = 0.523$ nm, $b = 9.06$ nm, $\alpha = \gamma = 90°$, $\beta = 99°$. Value c is not a constant and ranges from 0.960 to 1.85 nm based on the types of the exchangeable cations and the numbers of water molecules among the structure layers. A supercell is composed of 8 unit cells in the form of $4a \times 2b \times c$, and water molecules were inserted into the interlayers of the supercell. The molecular formula of such montmorillonite supercell can be written as $M_{0.75}$ $(H_2O)_n (Si_{7.75} Al_{0.25}) (Al_{3.5} Mg_{0.5}) O_{20} (OH)_4$; M represents Ca^{2+}, Mg^{2+}, and Na^+. The size of the supercell on XOY plane is 2.092 nm × 1.812 nm. On the basis of Loewenstein law, one in 32 Si^{4+} was replaced by Al^{3+}, and one in 8 Al^{3+} was replaced by Mg^{2+} in the supercell. The negative charges (-6 e) were compensated by the interlayer Na^+, Ca^{2+}, or Mg^{2+} ions after isomorphous substitution.

2.3 Simulation method

The materials science code Cerius[2] was employed to compute the clay mineral hydration. Energy minimization and dynamics simulations were processed in the C2 Minimizer and C2 Dynamics modules, and the universal force field (UFF) in C2. The OFF module was chosen. The long-range electrostatic interaction was computed by Ewald summation. Van der Waals force was computed by the LJ function, and its cut-off radius was 0.9 nm. The charge was calculated by using the charge equilibration (QEq) method. After energy optimization by UFF, dynamic simulation was performed on the montmorillonite crystal lattice with one, two, and three layers of water molecules (32, 64, and 96 water molecules, respectively) under the microcanonical ensemble and 300 K.

3 Results and Discussions

3.1 Mineral phase identification

Tab. 1 presents the chemical compositions of Nairobi BCS obtained by XRF and lists the literature data of the chemical composition of expansive soil in Ningming, China. BCS is characterized by a high iron (Fe_2O_3) content. The same characteristic was also found in India BCS. However, the iron content in Ningming soil is only 3.23%, which is far less than that in Nairobi BCS (9.44%). The literature previously established that the black color of the soils could be due to the presence of iron, manganese, and titanium in their reduced state. Nevertheless, the content of manganese and titanium in Nairobi BCS was only 0.3% and 0.9%, respectively. The high content of iron in its reduced state might be a principal factor in the dark color of Nairobi BCS. This finding is similar to previous findings.

However, the darkness of clay is generally believed to be caused by the abundance of organic carbon. Therefore, a test was performed by pouring 1 g of Nairobi BCS into 20 mL of 30% hydrogen peroxide solution to remove the organic matter from the soil (see Fig. 2). Organic matter in the soil is another factor that can contribute to the

Tab. 1 Chemical (oxide) composition of BCS and Ningming expansive soil %

Oxide content	$w(CaO)$	$w(MgO)$	$w(Fe_2O_3)$	$w(Al_2O_3)$	$w(SiO_2)$	$w(K_2O)$	$w(Na_2O)$	$w(SO_3)$	$w(P_2O_5)$	$w(MnO)$	$w(TiO_2)$	LOI
BCS	1.70	0.95	9.44	16.89	50.34	1.01	0.76	0.15	0.02	0.30	0.90	17.50
Ningming soil	0.20	1.45	3.23	27.59	55.45	3.07	0.16		0.17	0.02	0.33	7.35

Note: Data of Ningming soil were obtained from Ref. [14].

darkness of the BCS, as indicated by the comparison of the color change in 20 mL of 30% hydrogen peroxide solution and the water. Another noticeable characteristic of BCS is that the alkali content of CaO and Na_2O is about 8.5 and 5 times that of Ningming soil, respectively, while the content of K_2O is only about one-third that of Ningming soil. Hence, BCS is mainly composed of calcium- and sodium-based clay minerals, which presents higher expansibility than potassium-based clay minerals upon exposure to water.
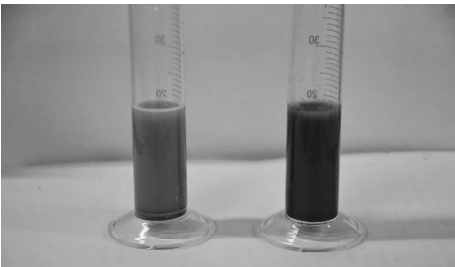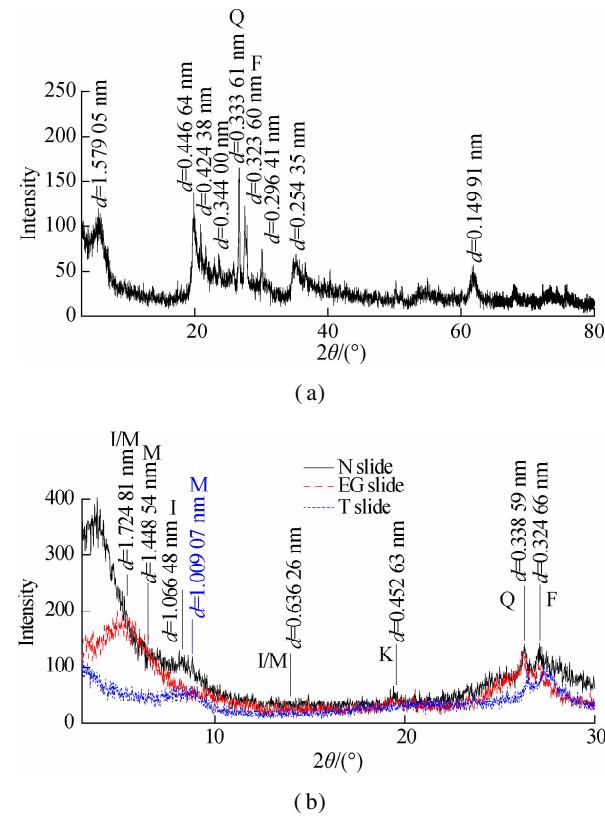

Fig. 2 1 g of BCS poured into 20 mL of 30% hydrogen peroxide solution (left) and distilled water (right)

Raw BCS particles on the glass slide were fixed on the X-ray measurements to primarily understand the mineral phases in BCS. Fig. 3(a) presents the XRD pattern of the untreated BCS. The basic reflection peak is found at about $d = 1.579\ 05$ nm, and its corresponding second- and multiple-harmonic peaks are obvious, thereby indicating the presence of periodical layered structures in BCS. The broader basic reflection peak also indicates the low crystallinity of those structures or the presence of mixed-layer minerals in BCS.

(a)

(b)

M—montmorillonite; I—illite; I/M—interstratified illite-montmorillonite; K—kaolinite; Q—quartz; F—feldspar

Fig. 3 XRD pattern. (a) Raw BCS; (b) Clays separated from BCS by suspension method recorded on the oriented slides after air drying (N), ethylene glycol saturation (EG), and heating at 550 ℃ (T)

The clays were coated on a glass slide for XRD measurements to further confirm the presence of clay minerals in BCS after air drying, ethylene glycol saturation, and heating at 550 ℃. As shown in Fig. 3(b), montmorillonite is detected by the reflection peak at $d = 1.448\ 54$ nm in the N slide, which moves to $d = 1.816\ 75$ nm in the pattern of clay saturated with ethylene glycol and collapses to $d = 1.009\ 07$ nm after heat treatment. Ca-based smectite is always found at about 0.015 nm, but Na-based smectite is found at 0.012 5 nm; that is to say, Ca-based montmorillonite is the main clay mineral in BCS. Moreover, a small number of clay minerals such as interstratified illite-montmorillonite, illite, and kaolinite with other non-clay minerals such as quartz and feldspar are detected in Nairobi BCS. To calculate the relative amount

of the clay minerals, overlapping peaks are resolved by using least-squares method, and curve fitting is performed by using the Lorentzian-Gaussian function. The proportion of montmorillonite, interstratified illite-montmorillonite, illite, and kaolinite is 32.6%, 10.9%, 2.3%, and 1.5%, respectively, according to the integration area. Moreover, a small amount of iron mineral phases such as goethite (0.6%) is determined in Nairobi BCS, which indicates that iron mainly exists in the form of clay minerals.

3.2 Hydration of interlayer cations

In general, the primary clay mineral in Nairobi BCS is montmorillonite with a small quantity of illite and kaolinite. Hence, the high expansive potential of Nairobi BCS mainly comes from the water swelling of montmorillonite. In addition, clays with different cation compositions and exchange capacities have a large difference in expansive potential. The CEC and exchangeable cations of Nairobi BCS and Ningming soil are presented in Tab. 2. The CEC of Ningming soil is 106.87 meq/100 g and is larger than that of Nairobi BCS, which is 58.3 meq/100 g. However, the FSR and FSI of Ningming soil are only 93% and 104%, respectively, which are lower than the FSR and FSI of Nairobi BCS, which are 121% and 168%, respectively. Nairobi BCS has a high content of Mg^{2+} and Na^+ with a percentage of up to 4.78% and 2.73%, respectively, and about 14 times that in the Ningming soil. These findings indicate that cation composition has a significant influence on the water absorption of montmorillonite. Hence, the montmorillonite crystal lattice with types of exchangeable cations in interlayers needs to be constructed to investigate the swelling properties of BCS.

Tab. 2 CEC and exchangeable cations of BCS samples

Test items	BCS	Ningming soil
CEC/(mmol · kg^{-1})	291.5	534.5
$w(Na)$/%	2.7	0.2
$w(Ca)$/%	47.1	93.7
$w(Mg)$/%	4.8	0.3
$w(K)$/%	1.6	2.6
δ_{FSR}/%	121.0	93.0
δ_{FSI}/%	168.0	104.0

Note: Data of Ningming soil were obtained from Ref. [15].

Tab. 3 presents the three montmorillonite structures, which are constructed to investigate the influence of Mg^{2+} and Na^+ on the swelling properties of montmorillonite. The supercell of Type Ⅲ montmorillonite without water molecules in interlayers is shown in Fig. 4. The pink octahedron represents the unsubstituted location of Al^{3+}; the green octahedron represents the location of Al^{3+} replaced by Mg^{2+}; the yellow tetrahedron represents the unsubstituted location of Si^{4+}; the pink tetrahedron represents the location of Si^{4+} replaced by Al^{3+}. The blue, green and

purple spheres represent Ca^{2+}, Mg^{2+}, and Na^+, respectively, which are used to balance the negative charges. The water molecule model is constructed on the Sketch atoms module and optimized on the Forceit module by using the SPC/E model and UFF.

Tab. 3 Construction of three montmorillonite structures

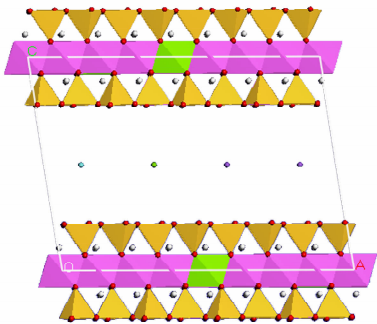| Configuration	Cations and percentage	Crystal texture
I	Ca^{2+} (100%)	$Ca_{0.375}^{2+}$ (H_2O)$_n$ ($Al_{3.5}$ $Mg_{0.5}$) ($Si_{7.75}Al_{0.25}$)O_{20}(OH)$_4$
II	Ca^{2+} (66.6%), Mg^{2+} (33.3%)	$Ca_{0.25}^{2+}$ $Mg_{0.125}^{2+}$ (H_2O)$_n$ ($Al_{3.5}$ $Mg_{0.5}$)($Si_{7.75}Al_{0.25}$)O_{20}(OH)$_4$
III	Ca^{2+} (33.3%), Mg^{2+} (33.3%), Na^+ (33.3%)	$Ca_{0.125}^{2+}$ $Mg_{0.125}^{2+}$ $Na_{0.125}^+$ (H_2O)$_n$ ($Al_{3.5}$ $Mg_{0.5}$) ($Si_{7.75}$ $Al_{0.25}$) O_{20} (OH)$_4$

Fig. 4 Supercell of Type III montmorillonite without the water molecule

The adsorption capability for water molecules of three types of montmorillonite was simulated on the Sorption module. Type III montmorillonite can adsorb 56 water molecules, which are larger than 51 and 53 water molecules of types I and II montmorillonite, respectively. A statistical analysis presented in Fig. 5 was performed on the distribution of adsorption energy for the water molecules of those two types of montmorillonite to further confirm the adsorption capability for water molecules of types I and III montmorillonite. Type III montmorillonite had a sharper distribution of adsorption energy, and the maximum and mean adsorption energy were 75 and 42 kJ/mol, respectively, but the values for Type I montmorillonite were 63 and 38 kJ/mol, respectively. The analyses indicate that Type III montmorillonite had stronger
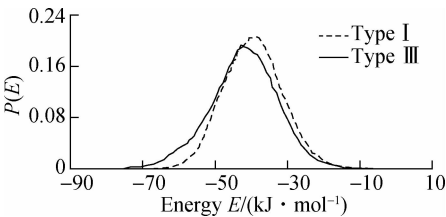

Fig. 5 Adsorption energy distribution curve of water molecules for types I and III montmorillonite

adsorption energy for water molecules and higher stability. The high expansive potential of Nairobi BCS comes from the strong adsorption capability for water molecules of montmorillonite with a high Mg^{2+} and Na^+ content.

The three types of montmorillonite with two layers of water molecules were investigated to compare the structural characteristics of the different types of montmorillonite with the same number of water molecules. If 1 kg of clay contains 0.1, 0.2, and 0.3 kg of water, then the distribution of water in montmorillonite is in the form of 1, 2, and 3 layers of water molecules, respectively, and the corresponding number of water molecules in the interlayer is 32, 64, and 96, respectively. The supercell of montmorillonite with two layers of water molecules can be obtained by inserting 64 water molecules into the interlayer. Fig. 6 presents the supercell of Type III montmorillonite with two-layer water molecules. After the structure optimization, molecular dynamics simulation was performed.
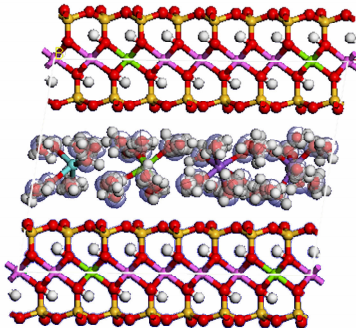

Fig. 6 Supercell of Type III montmorillonite with a two-layer water molecule

Fig. 7 shows the radical distribution function (RDF) of Ca^{2+}, Mg^{2+}, and Na^+ with Ow. The peak positions of Ca^{2+}/Mg^{2+}/Na^+-Ow RDF in types I, II, and III montmorillonite are shown in Tab. 4. The first peak of Na-Ow, Mg-Ow, and Ca-Ow RDF occurs near 0.222 5 nm, 0.227 5-0.242 5 nm, and 0.237 5-0.262 5 nm in types I, II, and III, montmorillonite, respectively. The difference of the first peak indicates that the positive ions have different capacities in organizing the oxygen atom. The Na-Ow RDF has a minimum first peak, which indicates that Na^+ has the strongest interaction with the oxygen atom and is easy to hydrate, and is then followed by Mg^{2+} and Ca^{2+} in order. Moreover, the distance between Mg^{2+}, Ca^{2+}, and Ow reduces obviously in Type III montmorillonite as compared with that in Type I and II montmorillonite. The small amount of Na + facilitates the hydration of Mg^{2+} and Ca^{2+} to some extent. The major exchangeable cation in the clay minerals of Nairobi BCS is Ca^{2+} with some amount of Mg^{2+} and a few Na^+. The Na^+ content is too small to be the compensation ion but can fa-

cilitate the hydration of Mg^{2+}, Ca^{2+}. Hence, the clay minerals of Nairobi BCS have a high expansive potential.
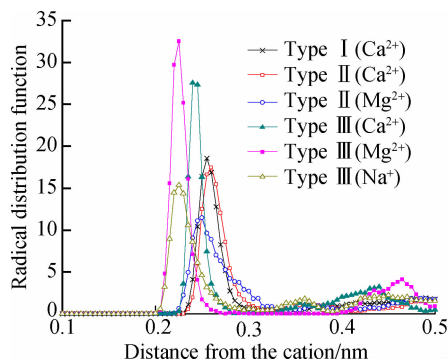

Fig. 7 Graphs of the $Ca^{2+}/Mg^{2+}/Na^{+}$-Ow RDF for montmorillonite hydrates

3.3 Identifying swell potential by FSI

The freeswell test of Nairobi BCS in the distilled water and kerosene was performed to estimate the rationalization of FSI as an index in determining the expansive potential of the clays. The expansive potential of the soils should be determined by the clay mineral content and the CEC because those two indexes can reflect the structural morphology and water adsorption capability, respectively. The FSI(FSR), CEC, and montmorillonite content were determined in the laboratory to verify the correlation of FSI with clay minerals and CEC.

The correlation of FSI and FSR with the montmorillonite content for Nairobi BCS is shown in Fig. 8. In the figure, M represents the content of montmorillonite in clay. The FSI presents a good correlation with the montmorillonite content of Nairobi BCS, having a positive linear correlation coefficient of $R^2 = 0.968\ 1$. However, the correlation of FSR with the montmorillonite content is relatively poorly qualified, and a positive linear correlation coefficient of $R^2 = 0.824\ 3$ is obtained. The correlation of FSI and FSR with CEC(C) for Nairobi BCS is shown in Fig. 9. A positive linear correlation coefficient of $R^2 = 0.941\ 6$ means that FSI has a good correlation with CEC of Nairobi BCS, indicating better performance than FSR,
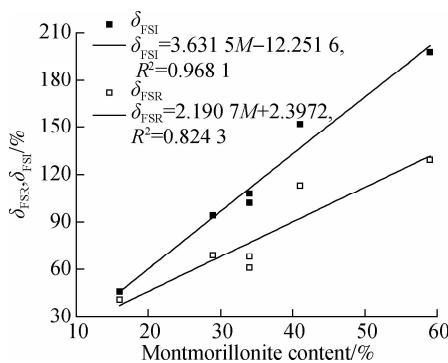

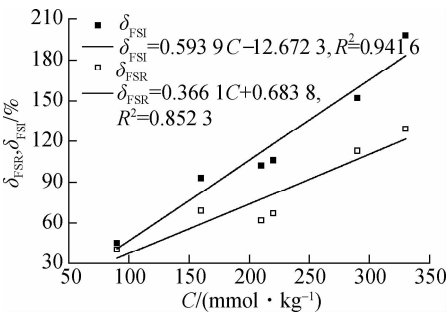**Fig. 8** Correlation of FSR/FSI with montmorillonite content for Nairobi BCS

Fig. 9 Correlation of FSR/FSI with CEC for Nairobi BCS

which has a positive linear correlation coefficient of $R^2 = 0.852\ 3$ with Nairobi BCS.

Overall, the FSI has a good linear correlation with intrinsic parameters that represent the swelling potential of the expansive soil for Nairobi BCS. Hence, FSI is ideally suited as a distinguishing index to determine the swelling potential of Nairobi BCS. Focused research has been conducted on the standards by using montmorillonite content and CEC as the classification indicators[16]. On the basis of the linear correlation of FSI with the montmorillonite content and CEC of Nairobi BCS, the criteria presented in Tab. 4 can be obtained by using FSI as a classification indicator.

Tab. 4 FSI criteria for identifying swelling potential

Swelling potential	$M/\%$ *	CEC/(mmol/kg) *	FSI/%
Non-expansive	< 7	< 85	< 25
Low	7 to 17	85 to 130	25 to 56
Moderate	17 to 27	130 to 180	56 to 90
High	> 27	> 180	> 90

Note: * Data were obtained from Ref. [16].

4 Conclusions

1) The high percentage of clay minerals, which are composed of montmorillonite (32.6%), interstratified illite-montmorillonite (10.9), illite (2.3%), and kaolinite (1.5%), is the major reason for the high expansive potential of Nairobi BCS.

2) The black color of Nairobi BCS is due to the presence of iron in its reduced state and organic carbon.

3) A limited number of Na^+ in BCS enhances the adsorption capacity for water molecules of montmorillonite and accelerates the hydration of Mg^{2+}, Ca^{2+} in clays, which ultimately leads to the high expansion of Nairobi BCS.

4) FSI presents a good linear correlation with the montmorillonite content and CEC, and it can be used as an index to classify the swelling potential of BCS.

References

[1] Patel S. Engineering properties of black cotton soil-dolime mix for its use as subbase material in pavements [J]. *International Journal of Geomate*, 2015, **8**(1):

1159 – 1166. DOI:10. 21660/2015. 15. 4191.

[2] Zhang P P, Huang J Q, Shen Z P, et al. Fired hollow clay bricks manufactured from black cotton soils and natural pozzolans in Kenya[J]. *Construction and Building Materials*, 2017, **141**: 435 – 441. DOI:10. 1016/j. conbuildmat. 2017. 03. 018.

[3] Noolu V, Mudavath H, Pillai R J, et al. Permanent deformation behaviour of black cotton soil treated with calcium carbide residue[J]. *Construction and Building Materials*, 2019, **223**: 441 – 449. DOI:10. 1016/j. conbuildmat. 2019. 07. 010.

[4] Gilbert B, Comolli L R, Tinnacher R M, et al. Formation and restacking of disordered smectite osmotic hydrates[J]. *Clays and Clay Minerals*, 2015, **63**(6): 432 – 442. DOI:10. 1346/ccmn. 2015. 0630602.

[5] Cheng Y Z, Huang X M, Li C, et al. Soil-atmosphere interaction as triggering factors of openings between embankment and pavement[J]. *KSCE Journal of Civil Engineering*, 2018, **22**(5): 1642 – 1650. DOI:10. 1007/s12205-017 – 0679-6.

[6] Nkalih Mefire A, Njoya A, Yongue Fouateu R, et al. Occurrences of Kaolin in Koutaba (west Cameroon): Mineralogical and physicochemical characterization for use in ceramic products[J]. *Clay Minerals*, 2015, **50**(5): 593 – 606. DOI:10. 1180/claymin. 2015. 050. 5. 04.

[7] Zhou C H, Zhao L Z, Wang A Q, et al. Current fundamental and applied research into clay minerals in China [J]. *Applied Clay Science*, 2016, **119**: 3 – 7. DOI:10. 1016/j. clay. 2015. 07. 043.

[8] Ammar M, Oueslati W, Ben Rhaiem H, et al. Quantitative XRD analysis of the dehydration-hydration performance of (Na$^+$, Cs$^+$) exchanged smectite[J]. *Desalination and Water Treatment*, 2014, **52**(22/23/24): 4314 – 4333. DOI:10. 1080/19443994. 2013. 803324.

[9] Jozanikohan G, Sahabi F, Norouzi G H, et al. Quantitative analysis of the clay minerals in the Shurijeh Reservoir Formation using combined X-ray analytical techniques [J]. *Russian Geology and Geophysics*, 2016, **57**(7): 1048 – 1063. DOI:10. 1016/j. rgg. 2016. 06. 005.

[10] Zheng Y, Zaoui A. Temperature effects on the diffusion of water and monovalent counterions in the hydrated montmorillonite[J]. *Physica A: Statistical Mechanics and Its Applications*, 2013, **392**(23): 5994 – 6001. DOI:10. 1016/j. physa. 2013. 07. 019.

[11] Ngouana W B F, Kalinichev A G. Structural arrangements of isomorphic substitutions in smectites: Molecular simulation of the swelling properties, interlayer structure, and dynamics of hydrated Cs-montmorillonite revisited with new clay models [J]. *The Journal of Physical Chemistry C*, 2014, **118**(24): 12758 – 12773. DOI:10. 1021/jp500538z.

[12] Research Institute of Highway Ministry of Transport. Test methods of soils for highway engineering: JTG E40— 2007 [S]. Beijing: China Communications Press, 2007. (in Chinese)

[13] National Energy Administration. Analysis method for clay minerals and ordinary non-clay minerals in sedimentary rocks by X-ray diffraction: SY/T 5163—2010[S]. Beijing: Petroleum Industry Press, 2010. (in Chinese)

[14] Li S L, Bo Z Z, Qin S J, et al. Application of plasitcity chart in distinguishing swelling soil[J]. *Geological Review*, 1984, **30**(4): 352 – 356. DOI: 10. 3321/j. issn: 0371-5736. 1984. 04. 007. (in Chinese)

[15] Tang H. *Research on swelling characteristics and treatment technology of black cotton soil in East Africa*[D]. Nanjing: Southeast University, 2017. (in Chinese)

[16] China Railway First Survey and Design Institute Group Co., Ltd. Code for special soil and rock investigation of railway engineering: TB 10038—2012 [S]. Beijing: China Railway Publishing House Co., Ltd., 2012. (in Chinese)

基于层间阳离子水化的黑棉土黏土矿物膨胀研究

程永振[1,2]　　黄晓明[1]

([1] 东南大学交通学院, 南京 210096)
([2] 淮阴工学院建筑工程学院, 淮安 223001)

摘要:为了分析黑棉土的吸水膨胀特性,采用 X 射线荧光光谱(XRF)和 X 射线衍射(XRD),测试了黑棉土的化学成分和矿物组成,应用 SPC/E 位能模型、UFF 力场、电荷平衡(QEq)算法和周期性边界,建立了蒙脱石晶胞模型,模拟了黏土矿物的层间阳离子水化. 结果表明,黑棉土中的黏土矿物主要为蒙脱石(32.6%),以及少量的伊/蒙混层矿物(10.9%)、伊利石(2.3%)和高岭石(1.5%). 黑棉土的高膨胀潜势来自于土壤中高镁离子含量和高钠离子含量的蒙脱石对水分子的强大吸附性能. 黑棉土中的交换性钠离子含量仅有3.73%,但其提高了黏土对水分子的吸附能力,并加速了镁离子(47.1%)和钙离子(4.78%)的水化. 差分自由膨胀率可以作为黑棉土胀缩潜势的分类指标.

关键词:黑棉土;膨胀特性;黏土矿物;分子模拟;层间阳离子水化

中图分类号:U416